Journal of Pharmaceutical and Biomedical Analysis 191 (2020) 113532

Contents lists available at ScienceDirect

Journal of Pharmaceutical and Biomedical Analysis

journal homepage: www.elsevier.com/locate/jpba

Determination of acid dissociation constants, enthalpy, entropy and Gibbs free energy of the baricitinib by the UV-metric and pH-metric analysis

Milan Meloun[a,*], Aneta Pfeiferová[a], Milan Javůrek[b], Tomáš Pekárek[c]

[a] Department of Analytical Chemistry, University of Pardubice, CZ 532 10 Pardubice, Czech Republic
[b] Department of Process Control, University of Pardubice, CZ 532 10 Pardubice, Czech Republic
[c] Zentiva, k.s., U Kabelovny 130, CZ 102 37 Prague, Czech Republic

ARTICLE INFO

Article history:
Received 25 May 2020
Received in revised form 3 August 2020
Accepted 3 August 2020
Available online 22 August 2020

Keywords:
Dissociation constants
Baricitinib
Spectrophotometric titration
pH-titration
REACTLAB
SQUAD84
ESAB

ABSTRACT

Baricitinib is a drug used for the treatment of rheumatoid arthritis. It is a selective and reversible inhibitor of Janus kinases 1 and 2, which play an important role in signalling the pro-inflammatory pathway activated in autoimmune disorders such as rheumatoid arthritis. The pH-spectrophotometric and pH-potentiometric titrations allowed the measurement of three or four successive dissociation constants of Baricitinib. Baricitinib neutral LH_2 molecule was able to protonate into two soluble cations LH_4^{2+}, LH_3^{+} and dissociate into two soluble anions LH^{-} and L^{2-} in pure water. The graph of molar absorption coefficients of differently protonated species *versus* wavelength indicated that the spectra ε_L, ε_{LH}, ε_{LH2} were the nearly the same for these species and that the spectra ε_{LH4} and ε_{LH3} were also similar. In the pH range from 2–13, four pK_aś of spectra analysis were reliably estimated by REACTLAB at I =0.0020 mol. dm^{-3} values pK^T_{a1} = 3.07, pK^T_{a2} = 3.87, pK^T_{a3} = 6.27, pK^T_{a4} = 12.78 at 25 °C and pK^T_{a1} = 3.00, pK^T_{a2} = 3.79, pK^T_{a3} = 6.12, pK^T_{a4} = 12.75 at 37 °C. Potentiometric pH-titration analysis for a higher concentration of 1 × 10^{-3} mol. dm^{-3} estimated with ESAB at I =0.0001 mol. dm^{-3} values pK^T_{a1} = 3.69, pK^T_{a2} = 3.81, pK^T_{a3} = 4.73 at 25 °C and pK^T_{a1} = 3.62, pK^T_{a2} = 3.73, pK^T_{a3} = 4.43 at 37 °C. Molar enthalpy ΔH°, molar entropy ΔS° and Gibbs free energy ΔG° were calculated from the spectra using a dependence ln K to 1/T.

1. Introduction

Baricitinib of the trade names Olumiant or Baricinix belongs to the class of organic compounds known as pyrrolo[2,3-*d*]pyrimidines and being developed by Incyte and Eli Lilly in 2016. These are aromatic heteropolycyclic compounds containing a pyrrolo(2,3-d)pyrimidine ring system, which are pyrrolopyrimidine isomers with the 3-ring nitrogen atoms at the 1-, 5-, and 7-positions (Fig. 1). On 23 April, 2018, the FDA Advisory Committee recommended the approval of 2 mg Baricitinib for the treatment of rheumatoid arthritis, but did not recommend the 4 mg dose for serious adverse events [1]. On 31 May 2018, the FDA approved Baricitinib for the treatment of adult patients with moderate to severe active rheumatoid arthritis, in patients who did not respond to one or more antagonist therapies.

Baricitinib has the IUPAC name of 2-[1-(ethanesulfonyl)-3-(4-(7H-pyrrolo[2,3-*d*]pyrimidin-4-yl)-1H-pyrazol-1-yl)azetidin-3-yl]acetonitrile of the chemical formula $C_{16}H_{17}N_7O_2S$ with a molar mass of 371.419 g/mol. It possesses the InChI Key XUZMWHLSFXCVMG-UHFFFAOYSA-N and its UNII is ISP4442I3Y. It is registered under the external ID codes INCB-028050 and LY-3009104, under the CAS number 1187594-09-7 and its PubChem CID is 44205240. It belongs to the Drug Classes of Antirheumatic Agents and in the Pharmacotherapeutic classes of Immunosuppressants. Among its predicted properties in literature is water solubility of 0.357 mg/ml and two dissociation constants pK_a (strongest acidic) 13.89 and pK_a (strongest basic) 3.91.

One of the most important physico-chemical properties of each drug are its dissociation constants pK_aś. Protonation equilibria and drug ionization are particularly important for predicting their behaviour under physiological conditions, since the ionization state strongly affects solubility at the application site [2–5].

1 The acid dissociation constant or ionization constant $pK_{a,i}$ of the acid LHj can be determined by a regression analysis of potentio-

* Corresponding author.
E-mail addresses: milan.meloun@upce.cz (M. Meloun), aneta.pfeiferova@student.upce.cz (A. Pfeiferová), milan.javurek@upce.cz (M. Javůrek), tomas.pekarek@zentiva.com (T. Pekárek).

https://doi.org/10.1016/j.jpba.2020.113532
0731-7085/

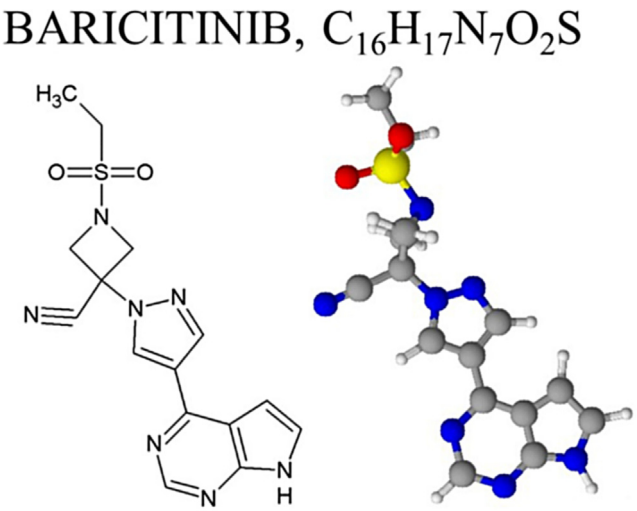

Fig. 1. The structural formula of Baricitinib.

metric titration data, also called the ***pH-metric analysis*** [6–9], in which the *common parameters* (pK_{ai}, i = 1,. . . ,j) and the *group parameters* (E^0, L_0, H_T) are simultaneously numerically estimated and refined [7]. We preferred using the regression program ESAB [7] for the potentiometric pH-titration data analysis.

2 The spectrophotometric ***UV-metric spectra analysis*** is a particularly highly sensitive and frequently used method of determining the acid dissociation constants or ionization constant pK^T_aś in very diluted aqueous solutions since it requires a relatively simple device and can work with low compound concentrations about 10^{-5} up to 10^{-6} mol. dm^{-3}, cf. [10].

3 To get an initial information about the number of dissociated protons and dissociation constants pK_aś the prediction of the protonation model from the structural formula of the drug molecule with the use of predictive programs ACD/pK [11] or ACD/Percepta [11,12], PALLAS [13] and MARVIN [14,15] was carried out.

The aim of this study was the UV-metric spectral analysis of the drug Baricitinib and alternatively the pH-metric analysis of the pH-titration curve of the protonation model to optimize experimental conditions so that all close successive dissociation constants could be reliably determined and to calculate three thermodynamic dissociation parameters such as the molar enthalpy ΔH°, the molar entropy ΔS° and the molar Gibbs free energy ΔG°. Detailed instructions for titrating the UV/VIS pH-absorption spectra, called UV-metric spectral analysis and alternatively pH-metric analysis, were previously described in their 10-steps procedure [15,16].

2. Materials and methods

2.1. Material

Baricitinib, donated by ZENTIVA, k. s., (Prague), had an HPLC-method declared purity and alkalimetry of always > 99%. This drug was weighed directly into a reaction vessel, resulting in a final analytical concentration that was expressed as äbout exactlyÏ.0 × 10^{-4} mol. dm^{-3}. *Hydrochloric acid*, 1.0 mol. dm^{-3}, was prepared by diluting concentrated HCl (p.a., Lachema Brno) with redistilled water and standardization against HgO with KI with a repeatability better than 0.002 mol. dm^{-3} according to HgO + 4 KI + H_2O ↔ 2 KOH + $K_2[HgI_4]$ and KOH + HCl↔KCl + H_2O. *Potassium hydroxide*, 1.0 mol. dm^{-3}, was prepared from the exact weight of the pellets (p. a., Aldrich Chemical Company) with carbon dioxide-free distilled water, which was pre-held for 50 min in an ultrasonic bath. The solution was stored for several days in a polyethylene bottle under an argon atmosphere and was standardized potentiometrically against a potassium hydrogen phthalate solution, and the equivalence point was evaluated using a derivative method with a reproducibility of 0.001 mol. dm^{-3}. *Mercury oxide, potassium iodide* and *potassium chloride* (p. a., Lachema Brno) were not subjected to extra purification. *Twice redistilled water* was kept for 50 min in a sonographic bath prior to the preparation of solutions.

2.2. Methods

The apparatus used and both titration procedures have been previously described in detail in our publications [15–17]. The free hydrogen ion concentration [H^+] was measured on a Hanna HI 3220 digital voltmeter with an accuracy of ±0.002 pH using a Theta HC 103-VFR combined glass electrode. Potentiometric titrations of the drug with potassium hydroxide were performed using an activity scale. Standardization of the pH meter was performed using standard WTW buffer values, 4.006 (4.024), 6.865 (6.841) and 9.180 (9.088) at 25 °C and 37 °C, in parentheses.

pH-spectrophotometric titration with absorbance spectrum registration at 300 wavelengths was performed as follows: an aqueous solution of 20.00 cm^3 containing 10^{-4} mol. dm^{-3} of drug, 0.100 mol. dm^{-3} of hydrochloric acid, 2.44 μmol. dm^{-3} phosphate buffer and 10 cm^3 of an indifferent ionic strength KCl solution was titrated with the standard 1.0 mol. dm^{-3} KOH at 25 °C and 37 °C and recorded 80 absorption spectra. Titrations were performed in a water-jacketed double-walled glass vessel of 100 cm^3 closed with a Teflon bung containing the electrodes, an argon inlet, a thermometer, a propeller stirrer and a hair capillary tip from a piston micro-burette [18]. All pH measurements were performed at 25.0 °C ± 0.1 °C and 37.0 °C ± 0.1 °C. During drug titration, the solution was bubbled through a stream of argon to thoroughly mix and maintain an inert atmosphere. The argon was passed through the aqueous ionic medium through two wash vessels which also contained the titration medium used before entering the corresponding titrand solution. The microburettes used with a total volume of 1250 μL (META, Brno) were equipped with a micrometer screw of 25.00 cm [18]. The hair polyethylene capillary of the microburette was immersed in the titrand solution during the titrant addition, but after each titrant addition, the microburette mouth was withdrawn to avoid spontaneous leakage of the titrant during the pH read-out. The microburette was calibrated by ten replicate determinations of the total volume of delivered water by weighing on a Sartorius 1712 MP8 balance with the results evaluated statistically resulting in an accuracy of ±0.015% of the added volume over the entire titration range. After each pH adjustment in the reaction vessel, the solution was transported to the cuvette by a peristaltic pump, which was part of a CINTRA 40 spectrophotometer (GBC, Australia) and then a spectrum at 300 wavelengths was recorded.

2.3. Software

Dissociation constants were estimated by the non-linear regression analysis of a set of 80 pH-absorbance spectra measured by UV-spectroscopy using two proven programs SQUAD84 [17,19] and REACTLAB [20]. The protonation model was then compared with its parameters and pH-metric analysis of the protonation modelś titration curve was conducted by ESAB [7]. Spectral interpretation of the factor analysis by quantifying the pH-absorbance matrix of the drug using the INDICES program [21] reliably determined the number of light-absorbing species n_c of the equilibrium mixture. Drug spectra plots were drawn with ORIGIN 9.1 [22]. The ACD/Percepta [11], PALLAS [13] and MARVIN [14] programs were used to predict the dissociation constants of pK_a and were always based on the structural formula of Baricitinib.

3. Results and discussion

Methods of numerical analysis of pH-spectra and pH-potentiometric titration curves have proven to be the best instrumental methods since they also reliably determine also close successive dissociation constants, even in the case of the poorly soluble drug Baricitinib. The pH-spectrophotometric titration by the *UV-metric spectral method* was used as an alternative method to the pH-potentiometric titration by the *pH-metric method* to determine dissociation constants in the case of larger molar absorption coefficients and showed high sensitivity to the drug concentration of Baricitinib 10^{-5} mol. dm^{-3} of the otherwise poorly soluble drug.

3.1. UV-metric spectral analysis

The experimental procedure and computational regression analysis strategy for determining dissociation constants by the *UV-metric spectral analysis* were described in the 10 steps in the published Tutorial [16] and can also be found on page 226 in the textbook [23]: Generally, the *Protonation model building and testing* concerns the following calculations: determining the number of protonation equilibriums, determining the number of differently protonated species, their representation in the relative concentration diagram as well as the construction of a graph of molar absorption coefficients *versus* the measured wavelengths of the protonation model.

Step 1: *Theoretical prediction of pK_a estimates from the Baricitinib structure:* The first step of the UV-metric spectral method was the prediction of the dissociation constant values, based on a quantum-chemical calculation, which is used on the structural formula of the drug molecule under study.

Baricitinib is an aromatic heteropolycyclic compound containing a pyrrolo (2,3-d) pyrimidine ring which is a pyrrolopyrimidine isomer with 3 nitrogen atoms at 1-, 5-, and 7-positions (Fig. 1). The prediction program MARVIN (denoted M) identified four protonatable centres in Baricitinib that could theoretically be associated with four predicted dissociation constants (Fig. 2). Both of the prediction programs, MARVIN and PALLAS (denoted P), predicted dissociation constants slightly differing from each other, so it was clear that the experimental determination of dissociation constants is necessary as it could generally offer more reliable results. Fig. 2a includes an overview of all predicted dissociation constants by the two programs M and P.

Figs. 2b to 2f illustrate a distribution diagram of differently protonated species and point to protonation centres in conjunction with the dissociation constant in question. Figs. 2d and 2e show two alternations of protonation centres in the dissociation constant pK_{a2} and their interpretation in the distribution diagram.

Step 2: *Number of light-absorbing species n_c:* Before the regression analysis of the pH-absorption spectra of the UV-metric spectral method, factor analysis was used to filter significant eigenvalues (SVD) of the second moment of the absorbance matrix to determine *the rank* of the absorbance matrix [21,24]. This factor analysis application was based on the fact that if the spectral data matrix consists of r contributions from light-absorbing chemical species, then the first r factors of the absorbance matrix contain the vast majority of the important chemical information obtained by the experiment. The value r then denoted the rank of the absorbance matrix and should generally be less than or equal to the number of light-absorbing differently protonated species m. Examination of the absorbance matrixś eigenvalues showed that the first factors were statistically significant up to the break on the Cattel index graph of eigenvalues from which the other estimated factors were already insignificant and might therefore be included in the experimental noise of the monitored absorbance. Since the change in the pH setting did not induce sufficient change in spectra and the spectra of some species were very similar, the break on the Cattel curve was not always unambiguous.

The Cattel eigenvalue index graph [24] (Fig. 3) showed that the whole matrix of Baricitinib pH-absorption spectra at 240−370 nm indicated three or four light-absorbing species in the equilibrium mixture $n_c = k^* = 3$ or 4 with the experimental noise level $s_k(A) = s_{inst}(A) = 0.28$ or 0.035 mAU. Furthermore, the spectra of the molar absorption coefficients of the first pair of species L^{2-} and LH- were shown to be very similar. The true number of light-absorbing species separated from spectral noise could also be reliably evaluated by non-linear regression analysis of spectral data in the building of a protonation model.

Step 3: *Building and testing the protonation model:* In the REACTLAB program, the non-linear regression analysis was used to process pH-absorbance spectra by the UV-metric spectral method using a regression triplet technique (*i.e.* data criticism, model criticism and numerical method criticism) cf. *ref.* [23,25–27].

The search for the best protonation model hypothesis with one, two, three and four dissociation constants was shown in the resulting molar absorption coefficient graphs and distribution diagrams of differently protonated species (Fig. 4) for the proposed protonation model hypothesis. The criterion for finding the best hypothesis of the regression model was the goodness-of-fit test of the calculated spectra by the experimental points of the pH-absorbance spectra, which was simplified here to calculate the standard deviation of the absorbance after the regression process $s(A) = \sqrt{RSS/(n - m)}$, where n was the number of absorbance points and m was the number of estimated parameters [25,27].

The construction of a protonation model [23] constituted a decision criterion for the acceptance of estimated parameters including its statistical diagnostics for the tested hypothesis. In the figure, this is in the form of the estimated standard deviation of the regression absorbance $s(A)$, which described the achieved fitness. The model with four dissociation constants proved to be the best protonation model since it reached the lowest value with $s(A) = 1.32$ mAU confirming the best fit. The curves of the molar absorption coefficients of the LH_2 and LH_3^+ species in the two pK model at $s(A) = 2.2$ mAU were nearly identical, for the LH_2, LH_3^+ and LH_4^{2+} species in the three pK model and at $s(A) = 1.9$ mAU near and for the L^{2-}, LH- and LH_2 species were almost identical in the four pK model and at $s(A) = 1.32$ mAU. It was shown that the building of the protonation model of Baricitinib was not an easy task, since this compound exhibited three close successive dissociation constants ($|pK_{a,i+1} - pK_{a,i}| < 3$) and the pH change during titration only slightly affected the absorbance of chromophores in spectra. Both dissociation constants were therefore poorly conditioned in the regression model and their determination was loaded with a higher degree of uncertainty.

Table 1 shows the numerical estimates of the dissociation constants calculated by the REACTLAB regression program with the residual mean $E|(\hat{e})|$ [mAU] and the residual standard deviation $s(\hat{e})$ [mAU] proved that the protonation model with four dissociation constants seemed to be the best one. The reliability of the calculated regression parameter estimates could also be tested by the following regression diagnostics (Table 1 and Fig. 4), as explained on page 226 in ref. [23].

(a) *Physical significance of estimates of unknown regression parameters:* The spectra of the molar absorption coefficients of differently protonated ε_L, ε_{LH}, ε_{LH2}, ε_{LH3}, ε_{LH4} of Baricitinib species *versus* wavelength were shown in the left part of Fig. 4. If in a pair of curves of molar absorption coefficients ε both values were close or almost the same, the protonation model hypothesis might be uncertain or even false.

(b) *Physical significance of species concentrations:* The distribution diagram of the relative concentrations of all species in the

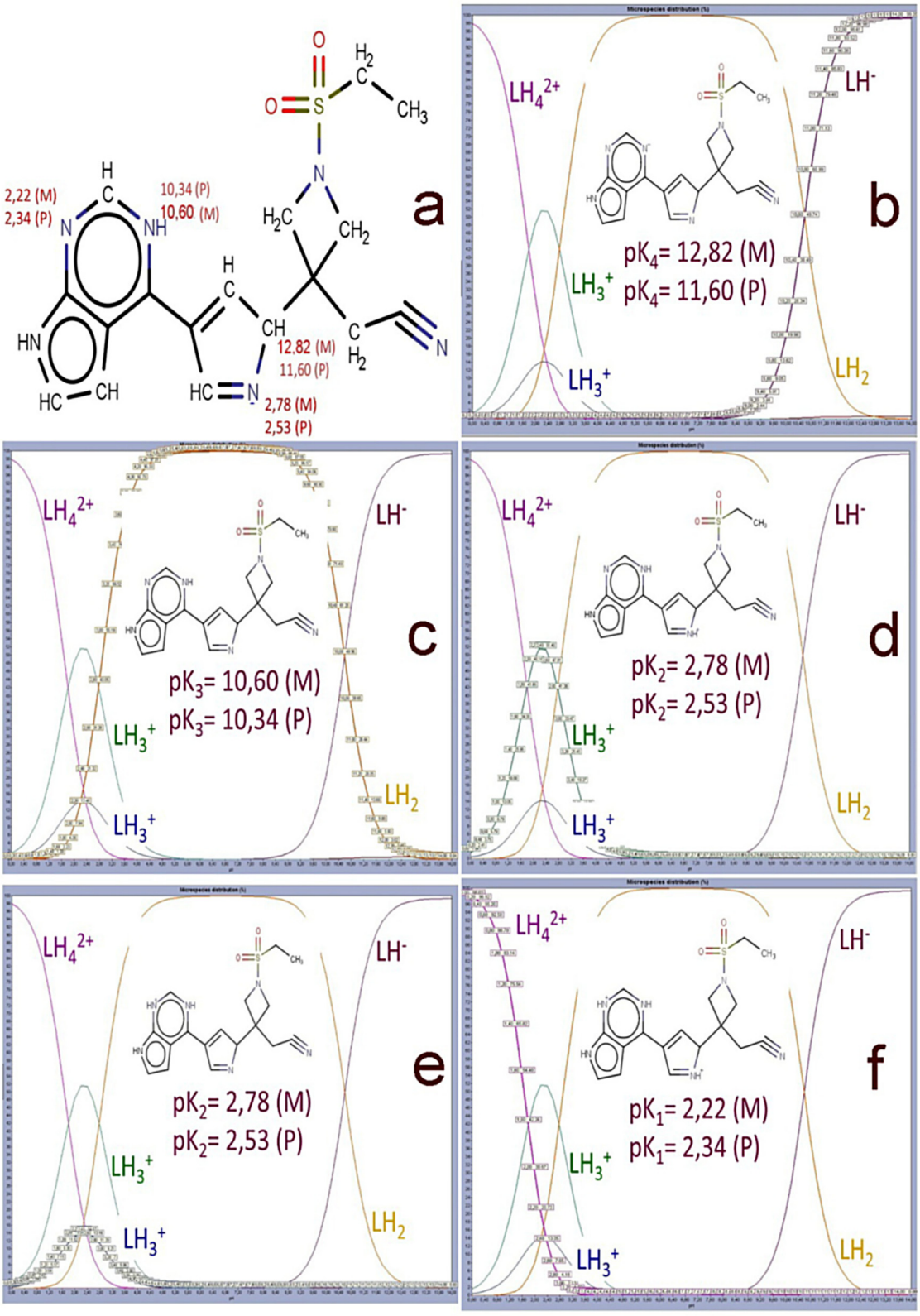

Fig. 2. The theoretical prediction of dissociation constants of Baricitinib is based on a structural formula and indicates (a) protonation centres showing predicted values of dissociation constants pK_a including the distribution diagram of relative concentrations of differently protonated species (b) LH^-, (c) LH_2, (d) LH_3^+, (e) LH_3^+, (f) LH_4^{2+} using programs MARVIN (M) and PALLAS (P).

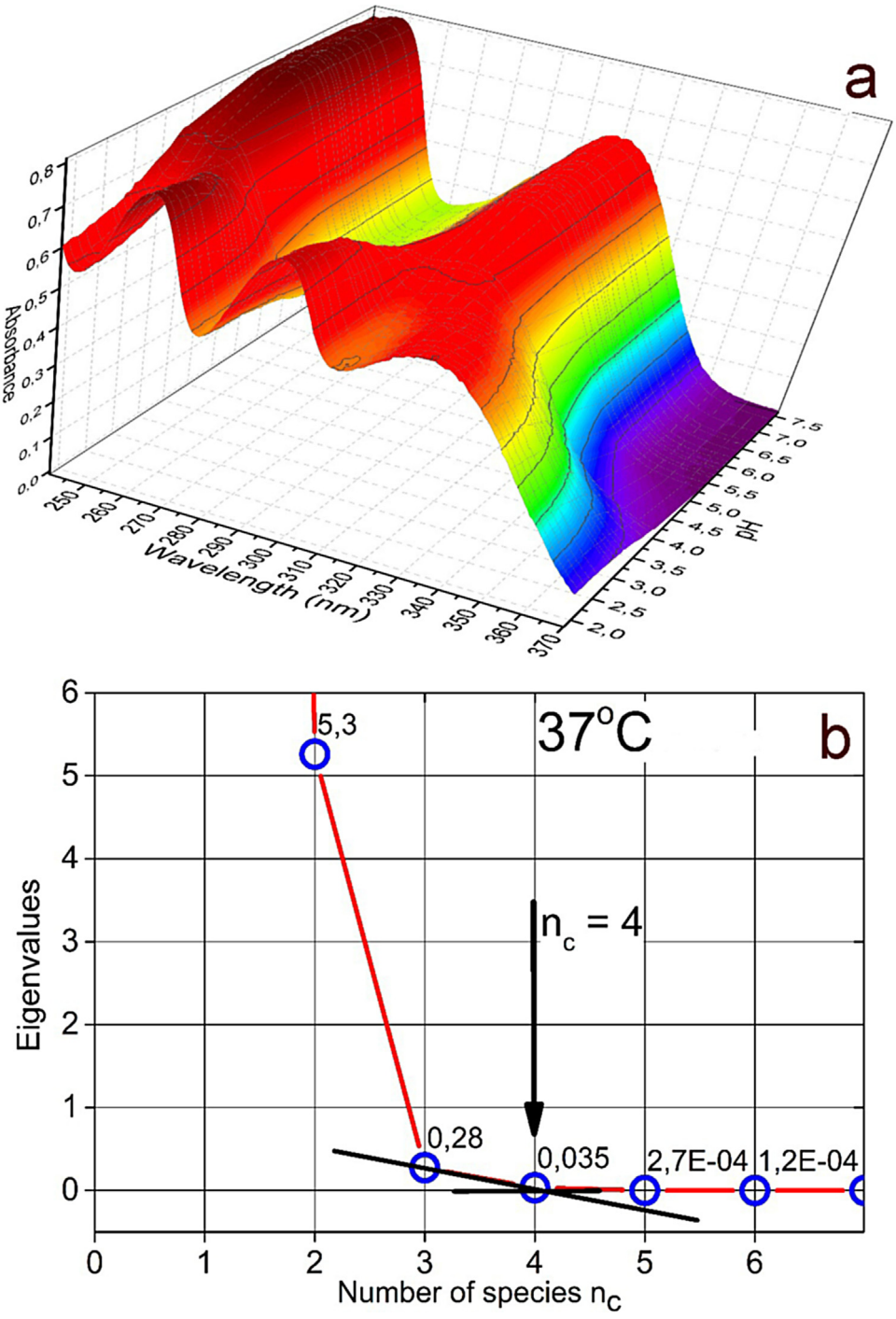

Fig. 3. The Cattel eigenvalue index graph shows the break of the eigenvalue curve of (a) the Baricitinib pH-absorbance matrix at 37 °C *versus* the factors corresponding to the matrix rank k^* = 3 or 4 and (b) the number of light-absorbing species n_c = 3 with $s_k(A)$ = 0.28 mAU or n_c = 4 with $s_k(A)$ = 0.035 mAU, where the residual standard deviation of absorbance and $s_k(A)$ is calculated with INDICES in S-PLUS.

right-hand part of Fig. 4 showed the protonation equilibrium of differently protonated species L^{2-}, LH-, LH_2, LH_3^+, LH_4^{2+} had physical meaning.

(c) *The goodness-of-fit test of calculated spectra:* The statistical analysis of all residuals showed that the minimum of the elliptic hyperparaboloid presenting the residual sum of squares of *RSS*-function was reached (Table 1) because the residual mean $E|(\hat{e})|$ [mAU] and the residual standard deviation $s(\hat{e})$ [mAU] reached very low values of less than 2 mAU, representing less than 0.2% of the absorbance measured.

Step 4: *Choice of the effective range of wavelengths* (Fig. S1 in Supplementary material): Four wavelength ranges (a) 230–370 nm, (b) 230–300 nm, (c) 240–290 nm and (d) 240–260 nm were selected and the spectra at these ranges were tested. Fig. S1 illustrated the reliability of the enumerated estimates of the four dissociation constants, including the goodness-of-fit of the spectra expressed as the standard deviation of the absorbance $s(A)$, which served here as the criterion for the reliability of the calculated parameter estimates. The best fit of the calculated spectra by experimental points with the fitness criterion of $s(A)$ = 0.62 mAU was achieved for the wavelength interval (d) 240−260 nm, although the estimates of

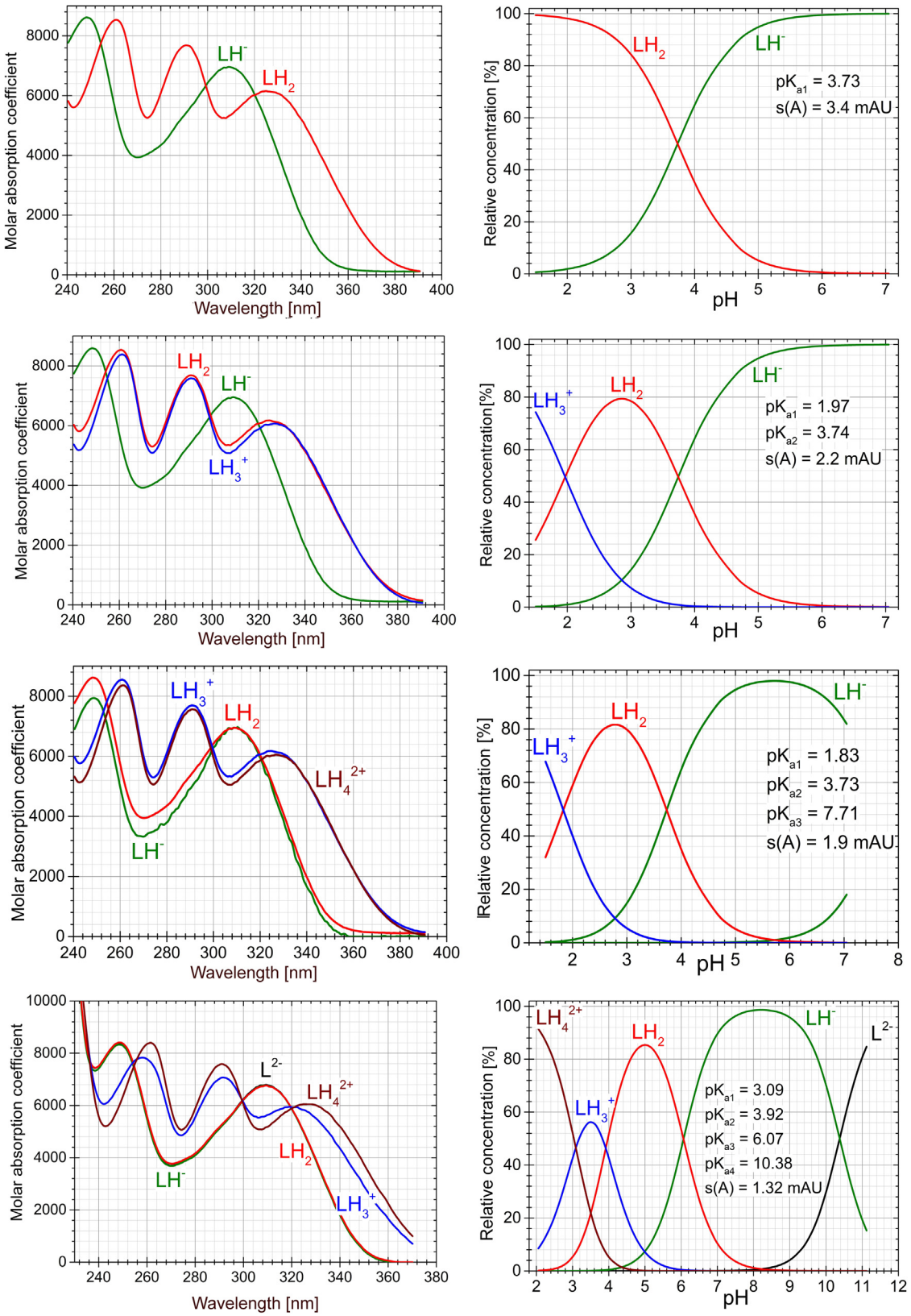

Fig. 4. The search of the best hypothesis of the tested proposed protonation model of Baricitinib in the pH range of 2 to 13 pointed to four dissociation constants pK_{a1}, pK_{a2}, pK_{a3} and pK_{a4} by spectral analysis of 1.0×10^{-4} mol. dm^{-3} Baricitinib at 25 °C. *Left:* Profiles of the molar absorption coefficients of differently protonated Baricitinib species ε_{LH}, ε_{LH2}, ε_{LH3}, ε_{LH4} *versus* wavelength (nm), *Right:* Distribution diagram of relative concentrations of differently protonated species in a protonation model *versus* pH (REACTLAB, ORIGIN 9).

Table 1
Reproducibility of the best protonation model of Baricitinib in the pH range of 2 to 13 for the four dissociation constants pK_{a1}, pK_{a2}, pK_{a3}, pK_{a4} using REACTLAB at 25 °C and 37 °C. Solutions of 1.0×10^{-4} M Baricitinib at I = 0.002 were used for n_s spectra, measured at n_w wavelengths form differently protonated species. The resolution criterion and reliability of the parameter estimates obtained are proven with the goodness-of-fit statistics of the residuals analysis such as the mean of absolute value of residuals $E|\bar{e}|$ [mAU], the standard deviation of the absorbance after the regression process $s(\hat{e})$ [mAU] and sigma $s(A)$ [mAU] from REACTLAB.

Temperature	25 °C					37 °C				
Reproducibility	1st set	2nd set	3rd set	4th set	Mean	1st set	2nd set	3rd set	4th set	Mean
Cattelś scree plot indicating the rank of the absorbance matrix (INDICES)										
Number of spectra, n_s	67	82	122	128		55	51	54	49	
Number of wavelengths, n_w	141	153	153	153		140	141	141	141	
Number of light-absorbing species, k^*	3	3	3	3		3	3	3	3	
Estimates of dissociation constants in the searched protonation model										
pK_{a1}, $LH_4^{2+} \rightleftharpoons H^+ + LH_3^+$	2.99	2.93	3.09	3.20	3.05	3.09	3.09	3.09	3.09	3.09
pK_{a2}, $LH_3^+ \rightleftharpoons H^+ + LH_2$	3.83	3.80	3.91	3.93	3.87	3.49	3.50	3.48	3.56	3.51
pK_{a3}, $LH_2 \rightleftharpoons H^+ + LH^-$	6.43	6.68	6.49	6.43	6.51	4.57	4.58	4.61	4.60	4.59
pK_{a4}, $LH^- \rightleftharpoons H^+ + L^{2-}$	12.19	12.30	12.34	12.63	12.37	12.65	12.88	12.89	12.92	12.84
Goodness-of-fit test with the statistical analysis of residuals										
Mean of absolute value of residuals, $E\|\hat{e}\|$[mAU]	0.78	0.9	0.94	1.02		1.4	1.5	1.65	1.66	
Residual standard deviation, $s(\hat{e})$, [mAU]	1.03	1.16	1.28	1.32		3.12	2.93	2.99	3.55	
Sigma from ReactLab, [mAU]	1.22	1.99	1.97	2.66		2.25	2.35	2.55	2.7	

the dissociation constants in all four wavelength ranges were close and nearly identical. Since the molar absorption coefficients of the species ε_{L2-}, ε_{LH-}, ε_{LH2} were almost identical in a significant number of wavelengths, this led to the conclusion that the pH change of the solution did not significantly affect the chromophores in question.

The determination of the dissociation constants pK_{a2} and pK_{a3}, and finally pK_{a4}, was loaded with considerable uncertainty, which was reflected in the higher standard deviation of the estimate of the dissociation constant pK_a, and therefore in its wider interval estimate. The close values of the two dissociation constants pK_{a1} and pK_{a2} also led to a minor difference in the spectra of the molar absorption coefficients ε_{LH3} and ε_{LH4}. A comparison of the four graphs in Fig. S1 (in Supplementary material), *i.e.* Fig. S1a, S1b, S1c, S1d showed that the region (d) of 240−260 nm appeared to be the most advantageous wavelength region of the spectrum for nonlinear regression analysis because it exhibited the best chromophore response to pH change.

Step 5: *The absorbance change in spectra within* **pH** *titration* (Fig. S2 in Supplementary materials): Fig. S2 showed the sensitivity of the chromophores in the Baricitinib molecule to the titration change in pH, which was monitored in the form of A-pH curves. The pH change did not always cause a significant change in the spectrum of Baricitinib at all wavelengths equally, as some chromophores were less affected by the pH change. Fig. S2c depicted the wavelength molar absorption coefficient spectrum for the nine selected wavelengths in Fig. S2a for which the A-pH curves of Fig. S2b have been shown. The maximum change in absorbance occurs here at pH changes around 340 nm and 260 nm. The graphs provided estimates of dissociation constants and the presence of differently protonated species. It was clear from these graphs that the two dissociation constants pK_{a1} = 3.09 and pK_{a2} = 3.92 were close and that their estimation was therefore loaded with greater uncertainty.

Step 6: *Signal-to-noise ratio in analysis of spectral changes* (Fig. S3 in Supplementary material): When spectrophotometric determination of the dissociation constants of Baricitinib was performed, it was necessary to investigate the hidden information in the spectral data to determine whether the titration change in pH caused a sufficient change in the spectral absorbance values for regression, to determine the dissociation constants and to build a protonation model. From Fig. S3 it was clear that the spectral response of the chromophore of the Baricitinib molecule (Figs. S3a and S3b) was not the same everywhere for all protonation equilibria, so it was necessary to investigate whether the four dissociation constants could be estimated at these minimal absorbance changes.

The change in the i-th spectrum of j-absorbance could be expressed by the magnitude of the difference $\Delta_{ij} = A_{ij} - A_i$ and then it was possible to investigate whether these changes were sufficiently large in the spectra and especially if they were greater than the noise value of the monitored absorbance in the $s_{inst}(A)$ spectrum. The changes of the absorbance difference Δ_{ij} [mAU] in the spectra were therefore plotted against the wavelength λ for all elements of the absorbance matrix (Fig. S3c) and it was shown that Δ_{ij} values in mAU were significantly greater than the instrument noise $s_{inst}(A)$ = 1–2 mAU.

Fig. S3d confirmed the excellent fitness of the calculated regression spectra through the experimental points, since the residual sizes e were predominantly in the range -5 to +5 mAU, while the changes in absorbance in the pH-spectral titration ranged from -350 to +350 mAU.

Step 7: *The spectra deconvolution* (Fig. S4 in Supplementary material): The deconvolution of each experimentally measured spectrum into the absorption bands of each differently protonated species [15–17] on Fig. S4 showed whether the protonation model hypothesis was designed efficiently and whether the spectra adequately reflected the protonation equilibria of Baricitinib. In addition, spectrum deconvolution appeared to be useful in analysing protonation equilibria, particularly in such exceptional cases where a change in the solutionś pH produced only a weak spectral response of the chromophore and therefore resulted in little or insufficient change in spectra. The molar absorption coefficient curves of the four differently protonated species in Fig. S4a showed that the curves of the LH_2, LH^- and L^{2-} species were almost identical, whereas there was a distinct difference between the curves of LH_4^{2+} and LH_3^+ and one neutral LH_2 molecule. The curves of the two protonated cations LH_4^{2+} and LH_3^+ were nearly identical. Therefore, special care in the interpretation of deconvolution had to be given a pH range of 3–6, since four LH_4^{2+}, LH_3^+, LH_2, LH- species were in equilibrium with three close dissociation constants pK_{a1} = 3.05, pK_{a2} = 3.87 and pK_{a3} = 6.51.

Fig. S4 illustrates the deconvolution of the experimental spectra at selected pH values, indicated by arrows to the pH axis in the distribution diagram of Fig. S4b, into the absorption bands of differently protonated Baricitinib species. At pH 2.14, the absorption band of LH_4^{2+} dominated in equilibrium with LH_3^+, which was still clearly distinguished. At pH 2.91, the spectra of the two cations LH_4^{2+} and LH_3^+ were very similar in shape, differing only by a slight shift. The pH range of 3–5 was very important, since there were present two cations LH_4^{2+} and LH_3^+ with one neutral LH_2 molecule in equilibrium. At pH 3.66, a spectrum of neutral species LH_2 appeared, which was different in shape from the spectra of

Table 2
Reproducibility of the best protonation model of Baricitinib in the pH range of 2 to 13 for the three dissociation constants pK_{a1}, pK_{a2}, pK_{a3} with ESAB was examined. The regression refinement of common and group parameters for pH-metric titration of acidified 1.0×10^{-3} mol. dm^{-3} Baricitinib was titrated with potassium hydroxide at 25.0 °C and 37.0 °C. The reliability of parameter estimation was proven with a goodness-of-fit statistics: the bias or arithmetic mean of residuals $E(\hat{e})$ [μL], the mean of absolute value of residuals, $E|\hat{e}|$ [μL], the standard deviation of residuals $s(\hat{e})$ [μL], the residual skewness $g_1(\hat{e})$ and the residual kurtosis $g_2(\hat{e})$ proving a Gaussian distribution, the Hamilton *R-factor* of relative fitness [%] from ESAB and the Akaike-Information Criterion *AIC*. *Common parameters refined:* pK_{a1}, pK_{a2}, pK_{a3}. *Group parameters refined:* H_0, H_T, L_0. *Constants:* t = 25.0 °C, 37.0 °C, pK_w = 13.9799, $s(V) = s_{inst}(y)$ = 0.1 μL, I_0 adjusted (in vessel), I_T = 0.9470 (in burette KOH).

Temperature	25 °C					37 °C				
Reproducibility	1st set	2nd set	3rd set	4rd set	Mean	1st set	2nd set	3rd set	4rd set	Mean
Estimates of the group parameters H_0, H_T and L_0 in the searched protonation model										
Number of points *n*	21	29	28	27		24	26	26	28	
$H_0 \times$ 1E + 02 [mol/L]	4.30	4.30	3.87	5.12		5.13	5.20	5.15	5.15	
H_T [mol/L]	0.9470	0.9470	0.9602	0.9602		0.9602	0.9602	0.9602	0.9602	
$L_0 \times$ 1E + 03 [mol/L]	0.34	0.37	0.99	0.36		0.28	0.29	0.29	0.28	
Estimates of the common parameters *i.e.* dissociation constants in the searched protonation model										
pK_{a1}. $LH_4^{2+} \rightleftharpoons H^+ + LH_3^+$	3.70	3.71	3.60	3.63	3.66	3.55	3.50	3.59	3.63	3.57
pK_{a2}. $LH_3^+ \rightleftharpoons H^+ + LH_2$	3.85	3.79	3.81	3.77	3.81	3.76	3.75	3.74	3.81	3.77
pK_{a3}. $LH_2 \rightleftharpoons H^+ + LH^-$	4.77	4.75	4.62	4.63	4.69	4.43	4.34	4.40	4.53	4.43
Goodness-of-fit test with the statistical analysis of residuals										
Bias or arithmetic mean of residuals $E(\hat{e})$. [μL]	−4.54E-08	−4.19E-08	−2.33E-07	−6.14E-08		−7.58E-10	3.94E-09	−2.72E-09	−3.97E-08	
Mean of absolute value of residuals. $E\|\hat{e}\|$[μL]	−6.44E-06	1.12E-05	3.80E-07	2.06E-05		6.20E-06	−4.67E-06	7.16E-06	6.02E-06	
Residual standard deviation. $s(\hat{e})$. [μL]	1.09E-04	1.11E-04	6.46E-05	8.83E-05		6.92E-05	7.92E-05	5.22E-05	9.43E-05	
Residual skewness $g_1(\hat{e})$	−0.75	−0.86	−1.25	−0.77		−0.62	−0.50	0.19	−0.17	
Residual kurtosis $g_2(\hat{e})$	4.03	4.17	6.45	3.25		3.40	3.63	2.41	3.14	
Akaike-Information Criterion. *AIC*	−363.80	−504.47	−509.54	−484.32		−441.7	−473.9	−497.7	−501.2	
Hamilton R-factor from ESAB [%]	0.02	0.02	0.01	0.01		0.01	0.01	0.01	0.01	

both previous cations. At pH 5.61, an LH^- anion spectrum appeared, which was similar to that of a neutral LH_2 species that increased with pH while the LH^- anion band decreased with pH and the spectrum of LH_3^+ cation almost disappeared. From pH 6.29, the LH^- anion band increased and the neutral LH_2 band decreased. At pH 11.12, the L^{2-} anion spectrum dominated and with LH^- the anion spectrum decreased.

3.2. pH-metric data analysis

Potentiometric titration of acidified Baricitinib to pH 2 titrated with potassium hydroxide was performed at 25 °C and 37 °C (Table 2) and at an adjusted ionic strength (Fig. 5). For pH-potentiometric titration by *the pH-metric method*, the estimation of each dissociation constant of Baricitinib was calculated by the ESAB regression program [7].

Step 8: *pH-metric data analysed by Bjerrum's formation function:* For the required "potentiometric" concentration, which was always higher than the concentration for spectrophotometric measurements, Baricitinib showed only three dissociation constants in the pH range of 3–6 and refined by nonlinear pH regression titration curves with ESAB. Non-linear regression analysis was applied to the central part of the pH-titration curve of acidified Baricitinib, titrated with potassium hydroxide. The protonated cations and anions of Baricitinib are soluble in the aqueous medium, while the neutral molecule is insoluble at pH > 7. Estimates of the three dissociation constants pK_{a1}, pK_{a2} and pK_{a3} were evaluated in the Bjerrum formation curve (Fig. 5a). At a pH greater than 7 and a concentration greater than 2×10^{-4} mol. dm^{-3}, a precipitate of the neutral molecule Baricitinib was formed.

Residuals were defined in the ESAB program as the difference between the experimental and calculated KOH titrant volume, $e_i = V_{exp,i} - V_{calc,i}$. The reliability test of the quantified estimates of the dissociation constants was performed by statistical analysis of residuals by the goodness-of-fit test. In addition to *the common parameters* pK_{a1}, pK_{a2} and pK_{a3}, and the subsequent refinement of *the group parameters* H_T, L_0, the goodness-of-fit test statistics improved significantly the best fit. The relatively sensitive reliability criterion of the estimated dissociation constants was the mean absolute value of residuals E|ē| expressed in μL. The comparison of the numerical value of this statistic with the instrumental noise of the microburette, $s_{inst}(V) = s(V)$ = 0.1 μL, proved to be a decisive criterion in the search for a regression model because the mean of absolute residual values $E|\bar{e}|$in μL and the residual standard deviation of the KOH titrant $s(V)$ were of the same size or even lower than the experimental microburette noise $s_{inst}(V)$. The values of both monitored statistics were 0.1 μL, which was close to the instrument error value of the microburettes used with $s(V)$ = 0.1 μL. In addition, the residuals varied between the lower limit -0.2 μL and the upper limit +0.2 μL of the Hoaglin interval, and no residual was outside these Hoaglin limits (cf. pages 29–34 in ref. [26] or page 474 in ref [25].). Estimation of the dissociation constants by ESAB was therefore considered to be sufficiently reliable (Table 2). The goodness-of-fit test of the calculated titration curve could only be improved by further refining the L_0 group parameter which is the Baricitinib drug concentration in the titration vessel.

Step 9: *Uncertainty of pK_{ai} in replicate measurements* (Fig. S5 in Supplementary material): The reproducibility of the dissociation constants evaluated by REACTLAB from four reproduced spectra measurements taken at different pH values was found to be in good agreement with the SQUAD84 estimates. The interpretation was as follows:

(a) The estimate of the mean pK_a and its variance from the reproduced dissociation constants served as a measure of uncertainty for each subsequent dissociation constant.
(b) At 37 °C, the estimates of the dissociation constant were slightly more acidic, *i.e.* lower pK_a values than the estimates at 25 °C.

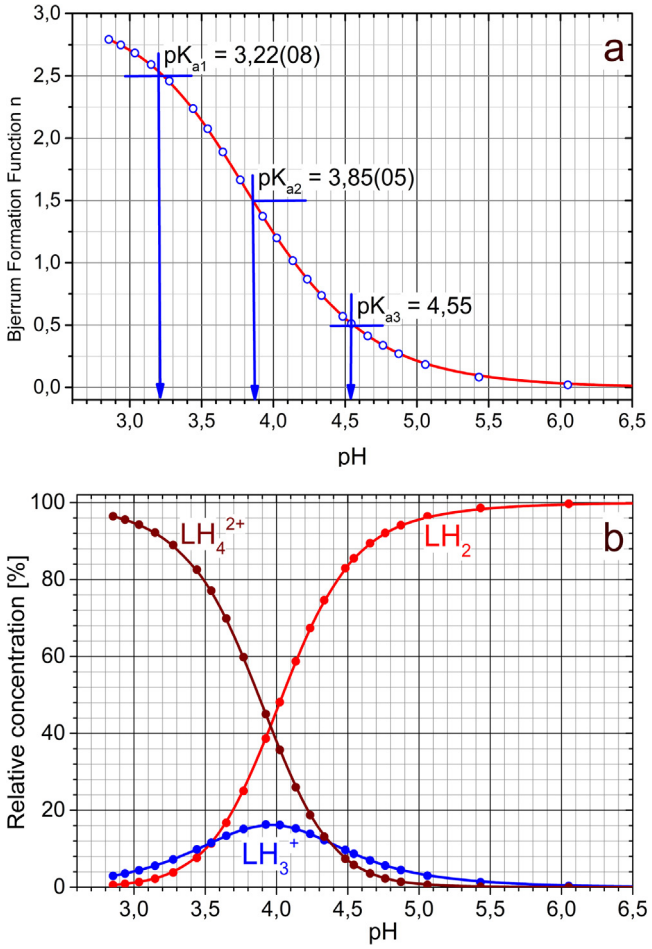

Fig. 5. (a) The pH-metric data analysed by Bjerrum's Formation Function of acidified Baricitinib to pH 2 titrated with potassium hydroxide at 25 °C indicates three dissociation constants in the pH range of 3 to 6. (b) Distribution diagram of the relative concentrations of variously protonated Baricitinib species in%.

(c) The close values of two consecutive dissociation constants pK_{a1} and pK_{a2} could lead to some difficulties in minimizing the process or could also cause their refinement values to fail in regression iterations. The reason could be an intermediate species that was not present at a sufficiently high concentration, or too close to pK_{a1} and pK_{a2}, and thus one species was highly correlated with its pK_a value with another species, and these species were formed at the same pH change.

(d) When the normal equations in the regression analysis were singular, one or more correlation coefficients between two parameters pK_{a1} and pK_{a2} were close to +1 or -1, the refinement process could be terminated prematurely by the program in the minimization process [25,27].

The reproducibility of dissociation constant estimates was also monitored potentiometrically at four temperatures from 25 °C to 50 °C. With increasing temperature, the values of all three dissociation constants decreased and thermodynamic parameters of ëxtratermodynamicsẅere evaluated from the slope of this linear dependence. Dissociation constants were determined from four repeated titration curves at each temperature and their mean value was calculated (Fig. S6 in Supplementary material).

Step 10: *Thermodynamic dissociation constants:* Using the Debye-Hückel low for the data in Tables 1 and 2, the unknown parameters of pK^T_{a1}, pK^T_{a2}, pK^T_{a3} and pK^T_{a4} were estimated at two temperatures of 25 °C and 37 °C. Due to the narrow range of ionic strength values treated, the effective ion size parameter *å* and the salinity coefficient *C* could not be calculated. *Spectrophotometry* (from mixed pK_a corrected to *I* =0.0020 mol. dm^{-3}): pK^T_{a1} = 3.07, pK^T_{a2} = 3.87, pK^T_{a3} = 6.27, pK^T_{a4} = 12.78 at 25 °C and pK^T_{a1} = 3.00, pK^T_{a2} = 3.79, pK^T_{a3} = 6.12, pK^T_{a4} = 12.75 at 37 °C. *Potentiometry* (from mixed pK_a corrections to *I* =0.0001 mol. dm^{-3}): pK^T_{a1} = 3.69, pK^T_{a2} = 3.81, pK^T_{a3} = 4.73 at 25 °C a pK^T_{a1} = 3.62, pK^T_{a2} = 3.73, pK^T_{a3} = 4.43 at 37 °C.

Step 11: *Determination of enthalpy, entropy, and Gibbs free energy for ẗhe extra-thermodynamicsöf dissociation:* The standard enthalpy change ΔH^0 of the dissociation process was calculated from the van't Hoff equation $d\ln K/dT = \Delta H^0/RT^2$. From the values of the standard molar Gibbs free energy $\Delta G^0 = -RT \ln K$ and enthalpy ΔH^0 we can calculate the standard entropy $\Delta S^0 = (\Delta H^0 - \Delta G^0)/T$, where R (ideal gas constant) = 8.314 J.mol^{-1}.K^{-1}, where *K* is the thermodynamic dissociation constant a *T* is the absolute temperature [28], (Fig. S7 and S8 in Supplementary material).

The literature [29] states that carboxylic and inorganic acids are least affected by temperature changes of less than ±0.05 pH units per 10 K, which is also related to minor changes in the molar enthalpy of dissociation close to 0. A clear correlation between dissociation enthalpy near 0 and lower p*K* sensitivity to temperature increase in carboxylic acids [29]. In contrast, phenols, amines and amino acids exhibit high enthalpy changes in the temperature range of 25–60 °C, with a change of -0.2 pH units to 10 K. The temperature change of the pK_a of the compound therefore changes the pH of the solution, which in turn may affect the solubility and chemical stability of the product.

The plot of the four dissociation constants p*K* at five temperatures by regression analysis of the spectra showed a slight decrease in p*K* with increasing temperature (Fig. S9-left). At higher concentrations of Baricitinib, precipitation of the drug occurred from pH above 7, initially only mild opalescence occurred, which made spectrophotometric indication impossible. Therefore, only the first three dissociation constants were evaluated potentiometrically as a function of temperature (Fig. S9-right).

For Baricitinib, with increasing temperatures ranging from 15 °C to 50 °C, the values of all four dissociation constants, determined spectrophotometrically (Fig. S9 left) and potentiometrically (Fig. S9 right), decrease. In the potentiometric pH-metric method, pK_{a1} decreased by 0.91 pH units with decreasing linear regression rabat R^2 = 98.44%, pK_{a2} decreased by 1.29 pH units with R^2 = 96.14% and pK_{a3} decreased by 1.07 pH units with R^2 = 93.12%, while the decrease in the estimation of the dissociation constants was lower for the UV-metric method, and therefore the slope of the temperature linear dependence was lower.

The temperature response of all three dissociation constants pK_{a1}, pK_{a2} and pK_{a3} was more pronounced in the potentiometric method, the correlation coefficients of the dissociation constant *versus* temperature were significantly higher than in the spectral method. The numerical estimates of the dissociation constants pK_{a1} and pK_{a2} determined by the potentiometric method were higher, or more alkaline, than the spectral method estimates, while pK_{a3} was the opposite. The chromophore response in the Baricitinib molecule was subject to somewhat greater uncertainty on the pH titration changes, resulting in worse reproducibility of the estimates of the dissociation constants from the spectra. In this respect, estimates of the three dissociation constants pK_{a1}, pK_{a2} and pK_{a3} appeared to be a more reliable method of pH-metric titration. The first dissociation constant of pK_{a1} was spectrophotometrically indicated as the estimated pK_{a1} parameter was very poorly conditioned in the regression model and therefore its estimation was loaded with greater uncertainty. Since pH-potentiometric titration required higher concentrations than the spectral method, it was not possible to determine the fourth dissociation constant of pK_{a4}, since Baricitinib precipitated at a pH greater than 7. Therefore, the

Table 3
The values of the thermodynamic dissociation constants at 25 °C and 37 °C, the standard molar enthalpy ΔH^0, the standard molar entropy ΔS^0 and the standard molar Gibbs free energy ΔG^0 determined with UV-metric spectra analysis and pH-metric analysis.

pK_a at 25 °C (and 37 °C)	ΔH^0 [kJ. mol^{-1}]	ΔS^0 [J. mol^{-1}]	ΔG^0 [kJ. mol^{-1} at 25 °C]
UV-metric spectra analysis			
$\mathbf{pK}^T_{a1}$ = 3.07 (3.00)	5.24	−40.31	12.02
$\mathbf{pK}^T_{a2}$ = 3.87 (3.79)	19.78	−6.56	1.98
$\mathbf{pK}^T_{a3}$ = 6.27 (6.12)	55.53	62.91	18.70
$\mathbf{pK}^T_{a4}$ = 12.78 (12.75)	23.78	−167.40	49.94
pH-metric analysis			
$\mathbf{pK}^T_{a1}$ = 3.69 (3.62)	41.91	69.58	21.09
$\mathbf{pK}^T_{a2}$ = 3.81 (3.73)	40.30	51.23	25.12
$\mathbf{pK}^T_{a3}$ = 4.73 (4.43)	18.54	−29.89	27.40

dissociation constant of pK_{a4} was determined only spectrophotometrically for 10-fold lower concentrations of Baricitinib.

Both parameters of linear dependence of p*K* on *T*, *i.e.* the intercept and the slope, were used for calculating thermodynamic quantities of enthalpy, entropy and Gibbs free energy (Fig. S9 and S10 in Supplementary material). The values of the standard molar enthalpy ΔH°, the standard molar entropy ΔS° and the standard molar Gibbs free energy ΔG° (Fig. S9 in Supplementary material) were calculated using the spectral method are in Table 3. The standard molar enthalpy values ΔH°, the standard molar entropy ΔS° and the standard molar Gibbs free energy ΔG° were also calculated by potentiometric titration are in Table 3. We know from published studies that positive enthalpy values $\Delta H^\circ(pK_{a1})$, $\Delta H^\circ(pK_{a2})$, $\Delta H^\circ(pK_{a3})$ and $\Delta H^\circ(pK_{a4})$ have shown that the dissociation process was endothermic and accompanied by heat absorption. The positive value of the standard molar Gibbs free energy $\Delta G^\circ(pK_{a1})$, $\Delta G^\circ(pK_{a2})$ and $\Delta G^\circ(pK_{a4})$ except for the negative $\Delta G^\circ(pK_{a3})$ monitored spectrophotometrically showed that the dissociation process was not spontaneous, while all ΔG° values were positive. Since the dissociation process entropy ΔS° (potentiometrically) was positive for two p*K*ś, namely $\Delta S^\circ(pK_{a1})$ = 69.58 J.mol^{-1} and $\Delta S^\circ(pK_{a2})$ = 51.23 J.mol^{-1} and with the spectrophotometry for one dissociation constant $\Delta S^\circ(pK_{a3})$ = 62.91 J.mol^{-1}, the dissociation process with positive entropy was indicated as irreversible. The entropy for the other three dissociation constants $\Delta S^\circ(pK_{a1})$ = -40.31 J.mol^{-1}, $\Delta S^\circ(pK_{a2})$ = -6.56 J.mol^{-1}, $\Delta S^\circ(pK_{a4})$ = -167.40 J.mol^{-1} (spectrophotometrically) and at the third dissociation constant $\Delta S^\circ(pK_{a3})$ = -29.89 J.mol^{-1} (potentiometricaly) was negative, indicating a reversible dissociation process.

The REACTLAB regression program analysed the pH-absorbance matrix of 1.0×10^{-4} mol. dm^{-3} of Baricitinib and calculated the estimates of the four dissociation constants by numerical procedures. The results of the refinement of the dissociation constant estimates are based on the minimum of the residual squares sum function *RSS*, the estimated parameters, the standard deviations of the parameters and correlation coefficients between them, the residuals map. When looking for a protonation model, it is usually necessary to carefully consider all these factors, since none of them alone was a reliable indicator of the success of the regression model.

The ESAB potentiometric pH-titration program, minimizing residuals $e_i = V_{exp,i} - V_{calc,i}$ reached a residual value of 0.1 or 0.2 μL, which means that an excellent fit of the calculated titration curve to the experimental points was achieved. It can be stated that the reliability of common parameters, *i.e.* the dissociation constants of Baricitinib, was proven, although the L_0, H_T group parameters were poorly conditioned in the regression model. The goodness-of-fit showed sufficient reliability of estimates of all three dissociation constants of Baricitinib at five different temperatures.

The disagreement of the experimentally calculated dissociation constants pK_{ai} with their theoretically predicted values from the structure of the Baricitinib molecule could be caused by the complex structure of the resonance of the heterocyclic nucleus and subsequently by different electron distributions, which apparently led to different theoretically predicted pK_{ai} values. In such cases, the MARVIN, PALLAS, and ACD/Percepta prognostic programs would fail somewhat and the dissociation constants would therefore be more plausible from the experimental determination. Since pK_{ai} estimates by both potentiometric and spectrophotometric methods were similar, and further considering the plausibility of regression data analysis, it could be concluded that the experimental results obtained are reliable and confirm the true protonation equilibria of Baricitinib. From a thermodynamic perspective, the following conclusions are given for the protonation scheme (Fig. S11 in Supplementary material):

1) If pK_a was positive, the standard free energy change ΔG^0 for the dissociation reaction was also positive.
2) Furthermore, a positive value of ΔH^0 indicates that the dissociation process was endothermic and was accompanied by heat absorption. The rearrangement of the hydrogen bonds could then be the basis for both ΔH^0 and ΔS^0 in the drug-proton molecule interactions and the relationship between ΔH^0 and ΔS^0 seemed plausible, indeed likely. The hydrogen bond as the central interaction between the drug molecule and the proton was also mechanically attractive. In water, hydrogen bonds form a network of continuous chains that dynamically change in a certain state. Since the dipole formed by shifting the electron away from the hydrogen proton, these chains form a sequence of mono- and di-poles, which were sensitive to the electrostatic potential of the drug and receptor molecules and provided a mechanism for the remote transfer of information from the drug to the receptor.
3) The contribution of entropy in these reactions was usually unfavourable ($\Delta S^0 < 0$). The ions in the aqueous solution tended to orient the surrounding water molecules, which oriented the solution and reduced entropy. The ionic contribution to entropy was partial molar entropy, which was often negative, especially for small or highly charged ions. Acid ionization involved the reversible formation of two ions, so that entropy decreased ($\Delta S^0 < 0$).

4. Conclusion

(1) Spectrophotometric and potentiometric pH titration allowed the measurement of up to three or four successive Baricitinib dissociation constants (Fig. S10 in Supplementary material). Baricitinib chromophores showed relatively small changes in absorbance in the UV/VIS-spectra when the pH of the solution was changed, and therefore the dissociation constant estimates were exposed to greater uncertainty than was the potentiometric assay. Therefore, the estimation of dissociation constants monitored potentiometrically seemed to be more reliable.

(2) Baricitinib LH_2 was able to protonate into two soluble cations LH_4^{2+}, LH_3^{+}, a neutral LH_2 molecule, and dissociate into two soluble anions LH^{-} and L^{2-} in pure water. The graph of molar absorption coefficients of these differently protonated species *versus* wavelength indicated that the spectra ε_L, ε_{LH}, ε_{LH2} were similar to the same for the species, and the spectra ε_{LH4} and ε_{LH3} were also similar.

(3) It has been shown that four dissociation constants from the spectra could be reliably estimated in the pH range of 2–13 for the concentration of poorly soluble Baricitinib 1.0×10^{-4} mol. dm^{-3}. Although the adjusted pH less influenced the changes in absorbance in the chromophore, four dissociation constants were reliably determined with REACTLAB at I =0.0020 mol. dm^{-3}: pK_{a1} = 3.01 ± 0.12, pK_{a2} = 3.85 ± 0.11, pK_{a3} = 6.58 ± 0.12, pK_{a4} = 12.47 ± 0.05 at 25 °C and pK_{a1} = 3.09 ± 0.12, pK_{a2} = 3.51 ± 0.10, pK_{a3} = 4.59 ± 0.12, pK_{a4} = 12.84 ± 0.07 at 37 °C.

(4) Only three dissociation constants of Baricitinib were determined by regression analysis of potentiometric pH titration curves for a concentration of 1.0×10^{-3} mol. dm^{-3} with ESAB at I =0.0001 mol. dm^{-3}: pK_{a1} = 3.68 ± 0.03, pK_{a2} = 3.80 ± 0.03, pK_{a3} = 4.72 ± 0.05 at 25 °C and pK_{a1} = 3.61 ± 0.08, pK_{a2} = 3.72 ± 0.06, pK_{a3} = 4.42 ± 0.14 at 37 °C.

(5) The prediction of the dissociation constants of Baricitinib was performed by MARVIN, PALLAS and ACD/Percepta programs mainly to determine the protonation sites in the Baricitinib molecule. When comparing three predictive and two experimental techniques, the prognostic programs sometimes differed in the estimation of pK_a.

(6) The thermodynamic dissociation constants of Baricitinib are in Table 3.

The thermodynamic parameters ΔH^0, ΔS^0 and ΔG^0 were calculated from the temperature change of the dissociation constants and are in Table 3.

Author statement

Relevance: This manuscript has not been previously published in any language and it is not under consideration by another journal. Up today, no spectra, no dissociation constants or no pH-distribution diagrams of the relative concentration of variously protonated ions of the drug Baricitinib have been published.

Scientific motivation: Knowledge of the possible ionization states of a pharmaceutical substance, embodied in pK_a, is vital for understanding properties essential to drug development.

Novelty: Baricitinib is used for the treatment of rheumatoid arthritis. It is a selective and reversible inhibitor of Janus kinases 1 and 2, which play an important role in signalling the pro-inflammatory pathway activated in autoimmune disorders such as rheumatoid arthritis.

Significance: Medicine and pharmacology need physical constants (spectra, dissociation constants, solubility, *etc.*) of newly introduced drugs.

Appendix A. Supplementary data

Supplementary material related to this article can be found, in the online version, at doi:https://doi.org/10.1016/j.jpba.2020.113532.

Declaration of Competing Interest

The authors report no declarations of interest.

References

[1] FDA Briefing Document Arthritis Advisory Committee Meeting, AAC Brief NDA 207924 (2018).
[2] R.N. Goldberg, N. Kishore, R.M. Lennen, Thermodynamic quantities for the ionization reactions of buffers, J. Phys. Chem. Ref. Data 31 (2) (2002) 231–370.
[3] P. Nowak, M. Woźniakiewicz, K. P, Application of capillary electrophoresis in determination of acid dissociation constant values, J. Chromatogr. A 1377 (2015) 1–12.
[4] J. Reijenga, A. van Hoof, A. van Loon, B. Teunissen, Development of methods for the determination of pKa values, Anal. Chem. Insights 8 (2013) 53–71.
[5] H.D. Williams, N.L. Trevaskis, S.A. Charman, R.M. Shankere, W.N. Charman, C.E. Pouton, C.J.H. Porter, Strategies to address low drug solubility in discovery and development, Pharmacol. Rev. 65 (1) (2013) 315–499.
[6] L. Alderighi, P. Gans, A. Lenco, D. Peters, A. Sabatini, A. Vacca, Hyperquad simulation and speciation (HySS): a utility program for the investigation of equilibria involving soluble and partially soluble species, Coord. Chem. Rev. 184 (1999) 311–318.
[7] C. De Stefano, P. Princi, C. Rigano, S. Sammartano, Computer analysis of equilibrium data in solution ESAB2M: an improved version of the ESAB program, Ann. Chim. (Rome, Italy) 77 (7-8) (1987) 643–675.
[8] P. Gans, A. Sabatini, A. Vacca, Investigation of equilibria in solution. Determination of equilibrium constants with the HYPERQUAD suite of programs, Talanta 43 (10) (1996) 1739–1753.
[9] P. Gans, A. Sabatini, A. Vacca, Hyperquad computer-program suite, Abstr. Pap. Am. Chem. S. 219 (2000), U763-U763.
[10] R.I. Allen, K.J. Box, J.E.A. Comer, C. Peake, K.Y. Tam, Multiwavelength spectrophotometric determination of acid dissociation constants of ionizable drugs, J. Pharm. Biomed. Anal. 17 (4-5) (1998) 699–712.
[11] ACD/pKa DB, Advanced Chemistry Development, Inc., Toronto, Ontario, Canada, Toronto, Ontario, Canada, p. pK prediction software.
[12] M. Meloun, T. Syrový, S. Bordovská, A. Vrána, Reliability and uncertainty in the estimation of pK (a) by least squares nonlinear regression analysis of multiwavelength spectrophotometric pH titration data, Anal. Bioanal. Chem. 387 (3) (2007) 941–955.
[13] W. Krotz-Vogel, H.C. Hoppe, The PALLAS parallel programming environment, Lect Notes Comput Sc 1332 (1997) 257–266.
[14] ChemAxon, MARVINSketch 16.5.2.0., 2013.
[15] M. Meloun, S. Bordovská, Benchmarking and validating algorithms that estimate pK(a) values of drugs based on their molecular structures, Anal. Bioanal. Chem. 389 (4) (2007) 1267–1281.
[16] M. Meloun, S. Bordovská, T. Syrový, A. Vrána, Tutorial on a chemical model building by least-squares non-linear regression of multiwavelength spectrophotometric pH-titration data, Anal. Chim. Acta 580 (1) (2006) 107–121.
[17] M. Meloun, Z. Ferenčíková, M. Javůrek, Reliability of dissociation constants and resolution capability of SQUAD(84) and SPECFIT/32 in the regression of multiwavelength spectrophotometric pH-titration data, Spectrochim. Acta A. Mol. Biomol. Spectrosc. 86 (2012) 305–314.
[18] M. Meloun, V. Říha, J. Žáček, Piston Microburette for dosing aggressive liquids, Chem. Listy 82 (7) (1988) 765–767.
[19] D.J. Leggett, W.A.E. McBryde, General computer program for the computation of stability constants from absorbance data, Anal. Chem. 47 (7) (1975) 1065–1070.
[20] M. Maeder, P. King, Determination of the reaction mechanism and fitting of equilibrium and/or rate constants, chemometrics in practical applications (Editor K. varmuza), InTech 2012 (2012).
[21] M. Meloun, J. Čapek, P. Mikšík, R.G. Brereton, Critical comparison of methods predicting the number of components in spectroscopic data, Anal. Chim. Acta 423 (1) (2000) 51–68.
[22] ORIGIN, OriginLab Corporation, One Roundhouse Plaza, Suite 303, Northampton, MA 01060, USA.
[23] M. Meloun, J. Havel, E. Högfeldt, Computation of Solution Equilibria: a Guide to Methods in Potentiometry, Extraction, and Spectrophotometry, Ellis Horwood, Chichester, England, 1988.
[24] J.J. Kankare, Computation of equilibrium constants for multicomponent systems from spectrophotometric data, Anal. Chem. 42 (12) (1970) 1322–1326.
[25] M. Meloun, J. Militký, Statistical Data Analysis: a Practical Guide, Complete With 1250 Exercises and Answer Key on CD, first ed., Woodhead Publishing Limited, 80 High street Sawstone Cambridge, CB22 3HJ, UK, New Delhi, Cambridge, Oxford, Philadelphia, 2011.
[26] M. Meloun, J. Militký, M. Forina, Chemometrics for analytical chemistry PC-Aided Statistical Data Analysis, Volume 1, Ellis Horwood, Chichester, 1992.
[27] M. Meloun, J. Militký, M. Forina, Chemometrics for analytical chemistry PC-Aided Regression and Related Methods, Volume 2, Ellis Horwood, Chichester, 1994.
[28] D.D. Perrin, The effect of temperature on pK values of organic bases, Aust. J. Chem. 17 (4) (1964) 484–488.
[29] H. Fukada, K. Takahashi, Enthalpy and heat capacity changes for the proton dissociation of various buffer components in 0.1 M potassium chloride, Proteins 33 (2) (1998) 159–166.